An Experimental Study on Three Dimensional Heat Transfer Characteristics of Simulated Electronic Chips

Seong-Yeon Yoo*, Jong-Hark Park* and Young-Man Kwark**

(Received June 28, 1995)

Naphthalene sublimation technique is employed to investigate three dimensional heat transfer characteristics of the simulated electronic chips. Experiments are performed for a single chip and chip arrays. In case of a single chip, local heat transfer coefficients on four surfaces of the chip are measured for various gap sizes and air velocities. Dramatic change of local heat transfer is seen on each surface of the chip, and gap size between chip and base plate is found to affect heat transfer significantly. In case of chip arrays, heat tranfer characteristics from two-dimensional array of rectangular modules and three-dimensional array of hexahedral modules are investigated. Chip location, gap between chip and base plate and streamwise chip spacing are varied. Chips with small gap have much larger heat transfer values than chips without gap. Fully developed behavior is found from the third row, but it slightly depends on flow conditions. Local and average heat transfer coefficients of three-dimensional modules are a little bit greater than those of two-dimensional modules. The differences in magnitude decrease as the longitudinal chip spacing decreases.

Key Words: Electronic Chip Cooling, Naphthalene Sublimation Technique, Three Dimensional Heat Transfer

Nomenclature

B : Height of simulated electronic chip
D : Mass diffusion coefficient of naphthalene vapor in the air
H : Height of the flow channel
h : Heat transfer coefficient
h_m : Mass transfer coefficient
L : Width of the simulated electronic chip
$\dot{m}$: Rate of mass transfer
Nu : Nusselt number
Pr : Prandtl number
Re : Reynolds number
S : Streamwise distance between chips
Sc : Schmidt number
Sh : Sherwood number
Δt : Sublimation depth of naphthalene
$\Delta \tau$: Total exposure time in the wind tunnel
ρ_s : Density of the solid naphthalene
$\rho_{v,\omega}$: Naphthalene vapor density on the surface

*Department of Mechanical Design Engineering, Chungnam National University, Taejon, 305-764, Korea
**Car Audio Division, Daewoo Electronics Co., Incheon, 403-040, Korea

1. Introduction

Basic understanding of the characteristics of fluid flow and heat transfer around electronic chips is very important to determine optimum chip configurations and to find reliable and efficient methods for the cooling of electronic components or equipments. Among several cooling technologies, developed so far, forced convective air cooling is the most popular method. When the heat is released by forced convection from electronic chips in a narrow printed circuit boared channel, complex flow phenomena - such as stagnation and acceleration on the front surface,

separation and reattachment on the top surface, wake or cavity flow near the rear surface - affect the heat transfer characteristics (Chyu and Natarajan, 1991). It is necessary to measure the local heat transfer coeffcients to investigate how these flow conditions influence heat transfer characteristics from electronic chips. Nevertheless, there were few studies in the literature (Peterson and Ortega (1990), Sparrow et. al. (1983)) that dealt with local heat transfer measurements in arrays of electronic chips.

In a complicated flow situation, it is very difficult to measure local heat transfer coefficients by conventional methods of heat transfer measurement. Goldstein et. al. (1990) showed that mass transfer experiments using the naphthalene sublimation technique were the effective way for measuring the local heat transfer distribution in a complex, three-dimensional flow region. In the present study, naphthalene sublimation technique is employed to measure the local and average mass transfer from electronic chips. Then, the mass transfer data are converted to their counterpart of the heat transfer process using the heat/mass transfer analogy. Automated sublimation depth measurement system is used to measure the distribution of the local mass transfer, and precision balance is used for overall average mass transfer measurements.

Experiments are performed for a single chip and chip arrays. In case of a single chip, effect of the gap between chip and base plate on heat transfer is examined at various air velocities. Four surfaces of rectangular chip are casted with naphthalene. Array of three-dimensional electronic modules have frequently been treated as two-dimensional rectangular modules in the numerical and experimental studies because of its simplicity. Both modules, two-dimensional array of rectangular module and three-dimensional array of hexahedral module are tested in this study, and their local and average heat transfer coefficients are compared each other. Chip location, gap between chip and base plate, and streamwise chip spacing are varied for two-dimensional modules, and chip location and chip spacing are varied for three-dimensional modules.

2. Heat Transfer Measurement Using the Naphthalene Sublimation Technique

It has long been recognized that the convective heat transfer and the convective mass transfer can be considered as analogous processes. The governing equations for the convective heat and mass transfer processes clearly have the same expression. Thus, for a given configuration, if the thermal and concentration boundary conditions are the same and if $Pr_t = Sc_t$ (or laminar flow), the temperature and mass concentration fields are identical.

The following empirical correlation is often used for the forced convective heat transfer.

$$Nu = C\, Re^m Pr^n \tag{1}$$

Similar expression can be written for the forced convective mass transfer.

$$Sh = C\, Re^m Sc^n \tag{2}$$

Eq. (1) divided by Eq. (2) yields

$$Nu/Sh = (hB/k)/(h_mB/D) = (Pr/Sc)^n \tag{3}$$

The measured mass transfer coefficients or Sherwood numbers are converted to their counterpart of heat transfer using the above analogy relation. Yoo et. al. (1993) studied how geometries and flow conditions incorporate heat/mass transfer analogy.

2.1 Local mass transfer

Among various mass transfer experiments, naphthalene sublimation technique is used in this study. The model casted with naphthalene on the surface, is exposed to air in the wind tunnel. Naphthalene surface profiles are measured by the precise depth gage before and after exposure in the wind tunnel. Then, the mass transfer coefficient can be determined from

$$h_m = \rho_s \Delta t / \rho_{v,w} \Delta \tau \tag{4}$$

where ρ_s is the density of the solid naphthalene, $\rho_{v,w}$ is the naphthalene vapor density on the surface, Δt is the net sublimation depth, and $\Delta \tau$

is the total exposure time in the wind tunnel. Total naphthalene sublimation depth is calculated from the variation in measured surface elevations before and after the exposure, and the excess sublimation due to natural convection during the sublimation depth measurement period is subtracted from the total sublimation. The empirical equation of Ambrose et. al. (1975) is used to determine the naphthalene vapor pressure. From the ideal gas law, naphthalene vapor density on the surface is then evaluated. The Sherwood number can be expressed as,

$$Sh = h_m B/D \tag{5}$$

where B is the height of the simulated electronic chip. The mass diffusion coefficient of naphthalene in air, D, is determined from the Cho's (1989) correlation.

2.2 Overall mass transfer

The overall average mass transfer rate is determined by weighing total mass of test piece before and after exposure in the wind tunnel. This method has small measuring error and little natural convection loss during the measurement because it takes little time. The naphthalene sublimation rate is obtained from

$$\dot{m}/A = (\Delta m/A)/\Delta\tau \tag{6}$$

and the mass transfer coefficient is defined by

$$\dot{m}/A = h_m(\rho_{v,w} - \rho_\infty) \tag{7}$$

where A is total naphthalene casted area and ρ_∞, naphthalene vapor density in the freestream is zero. Combining Eqs. (6) and (7) gives

$$h_m = (\Delta m/A)/\rho_{v,w}\Delta\tau \tag{8}$$

3. Experimental Apparatus and Procedure

3.1 Experimental apparatus

The experimental apparatus comprises a wind tunnel, a naphthalene casting facilities, an automated sublimation depth measurement system and a precision balance. An open-circuit, blowing-type wind tunnel is used, which has square test section 300mm wide X 300mm high. Maximum air speed of the wind tunnel is 33m/s and the freestream turbulence intensity is less than 0.5% over the entire range of speeds.

The automated sublimation depth measurement system consists of a depth gage along with a signal conditioner, two stepper-motor driven positioners, a hardware unit for motor control and a personal computer. The depth gage used to measure the naphthalene surface profile is a linear variable differential transformer (LVDT; Schaevitz Engineering PCA-220-010), which has 0.254mm (0.01in) linear range and 25.4nm (1min) resolution. It is connected to a signal conditioner (Schaevitz DTR-451) which supplies excitation and converts the AC signal output of the depth gage to a DC voltage. For precise positioning, a system with two single-axis, lead-screw driven, perpendicularly located positioners is installed. This system can locate the depth gage on the naphthalene surface by controlling combined movements of each positioner. The stepper motors move the positioners with 0.0254mm (0.001in) per step. A personal computer with data acquisition board controls the movements of stepper-motors and reads the data from the signal conditioner.

Precision balance used to measure the overall average mass transfer is Satorius analytic balance with a resolution of 0.1mg and a capacity of 120g.

3.2 Procedure

A new naphthalene casting is made for each test run. The testpiece is clamped to a highly polished mold. Molten naphthalene is then poured into the mold. After the naphthalene solidifies and the system cools down to room temperature, the mold is separated from the testpiece by applying a shear force. The testpieces are placed and clamped on the measurement table. Initial readings of the naphthalene surface elevation are taken at predetermined locations using the automated sublimation depth measurement system. The nearest measurement location from the edge of the chip is 1.5mm for the top and bottom surfaces, and 0.5mm for the front and rear surfaces. The testpieces are then installed in the wind tunnel and exposed to the air stream for about one hour. During a test run, the naphthalene

surface temperature, tunnel air temperature and pressure and freestream velocity are measured. The testpieces are then removed and a second set of surface elevation is obtained at the same locations as before. Data reduction program calculate Sherwood numbers and Nusselt numbers based on the chip height, B, from the measured sublimation data.

4. Results and Discussion

Experiments are performed for single chip, two-dimensional chip array and three-dimensional chip array. Local and overall average mass transfer data are collected and converted to the heat transfer data using the heat/mass trnasfer analogy.

4.1 Single chip

Rectangular bar, having side length of 10× 30mm and 300mm long, is used for single chip measurements. Four surfaces in the middle section of the testpiece are machined with 1.5mm deep and 76mm long to hold naphthalene(Fig. 1). It is installed in the wind tunnel as shown in Fig. 2. Air velocity and gap size between chip and base plate of wind tunnel are varied and other dimensions are held fixed.

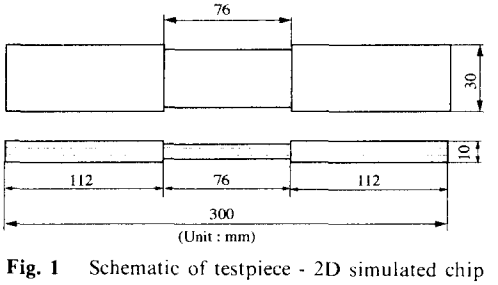

Fig. 1 Schematic of testpiece - 2D simulated chip

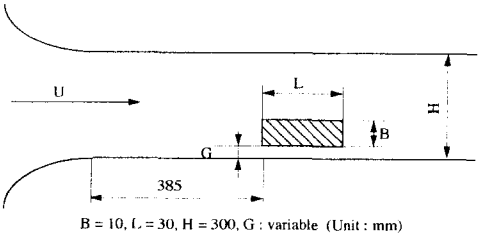

Fig. 2 Single chip installed in the wind tunnel

Distribution of local heat transfer rates on each surface of chip is shown in Fig. 3 for various gap sizes. When the chip is located far from the base plate (middle in the wind tunnel), mainstream boundary layer does not affect heat transfer from the chip, so distribution of the Nusselt numbers is symmetric. As the gap size decreases, dramatic change of the local heat transfer values is seen on each surface of the chip. Near bottom edge of the front face and on the bottom face, Nusselt numbers decrease rapidly with decreased gap size because of flow restriction between the chip and the base plate. Local maxima on the bottom surface are considered to be reattachment point of the separated flow. On the other hand, variation of Nusselt numbers on the top surface is quite complicate. In the position of the chip, mainstream boundary layer thickness is 7.7mm, 6.5mm and 5.9mm for the inlet velocity of 5m/s, 10m/s and 15m/s, repectively. In case of small gap size (less than 5mm in this study), a part of the chip is immersed inside the mainstream boundary layer, so boundary layer flow interacts with the chip. This interaction changes the flow pattern and heat transfer characteristics around the chip. When the gap size is greater than mainstream boundary layer thickness, boundary layer flow influences heat transfer only on the bottom surface of the chip. Figure 4 presents the distribution of local heat transfer rates for various air velocities in the case of G=5mm. Variation pattern is similar regardless of air velocity and Nusselt

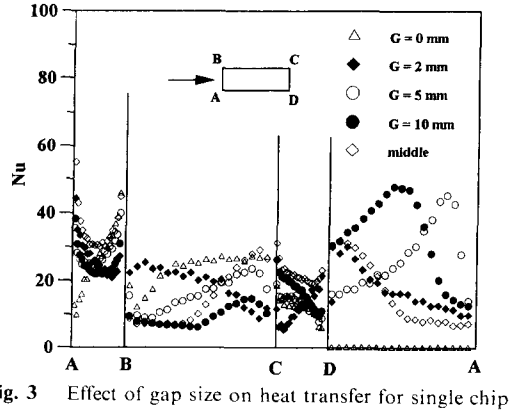

Fig. 3 Effect of gap size on heat transfer for single chip (u=5m/s)

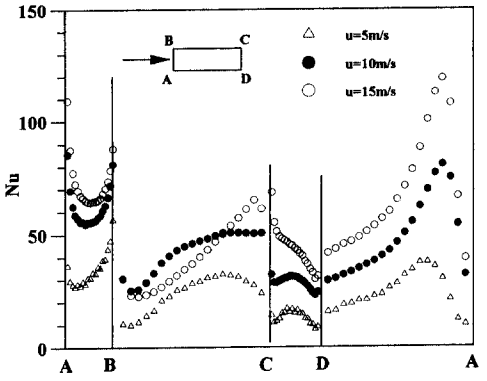

Fig. 4 Effect of inlet velocity on heat tranfer for single chip(G=5mm)

numbers increase as the air velocty increases. But, on the top surface, Nusselt numbers at air velocity of 15m/s is lower than those of 10m/s. This phenomena is related to the interaction of boundary layer flow with the chip.

Dependence of average Nusselt number on Reynolds number based on the chip height is presented in Fig. 5. The average Nusselt numbers are calculated by integrating the local Nusselt numbers for the surface area casted with naphthalene. The overall average Nusselt numbers increase as the Reynolds number increases regardless of gap size, but the dependence on Reynolds number is varied with gap size. On the top surface of some cases, average Nusselt numbers decrease at high Reynolds number. As shown previous figure, this is due to the interaction of the mainstream boundary layer flow with the chip.

4.2 Chip array

Test channel is installed in the middle of the wind tunnel for the experiments of chip array as shown in Fig. 6. The channel, which is made of 10mm thick arcryl, is 300mm wide, 40mm high and 450mm long. For the measurement of two-dimensional chip array, four rectangular bars are mounted on the bottom plate of the channel. One of them is naphthalene casted chip and the others are dummy chips. Naphthalene active chip is the same one that is used in single chip measurements. Location of naphthalene active chip, chip spacing (S), gap size (G) and air velocity are varied. Air velocity is measured using the pitot tube at 5mm downstream from the channel inlet.

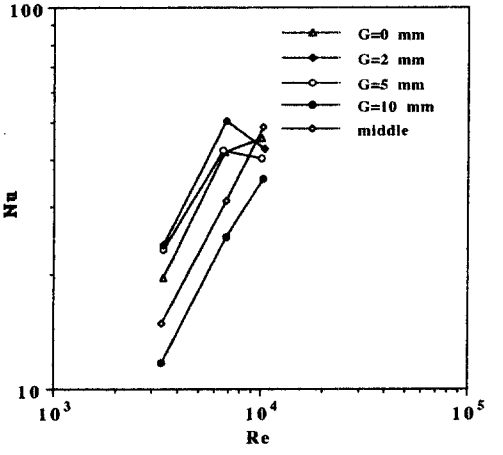

(a) Top

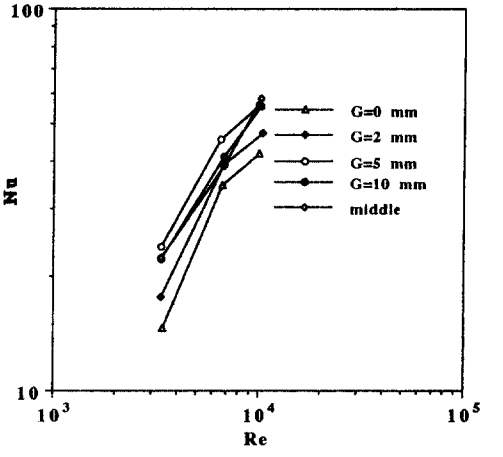

(b) Overall

Fig. 5 Dependence of average Nusselt number on Reynolds number for single chip

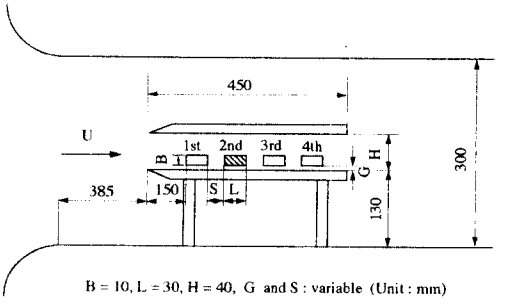

B = 10, L = 30, H = 40, G and S : variable (Unit : mm)

Fig. 6 Two-dimensional chip array installed in the flow channel and wind tunnel

Variation of local heat transfer distribution with the chip location is presented in Fig. 7. Heat transfer rates in the chips of the second and all subsequent rows are almost same each other, but their variation trends are much different from those of first row. In the situation without gap, fully developed behavior can be assumed from the third row. But, in the case of G=5mm, fully developed flow can be achieved far downstream. As can be seen in Fig. 8, heat transfer rates on the chip of third row increase monotonically with increased velocity. Same is true for G=5mm. This is somewhat different from the single chip measurement of Fig. 4, in which boundary layer interaction with the chip occurs.

Table 1 shows the average heat transfer on each surface of chip and the overall average for various gap sizes and chip locations. The value in the parenthesis denotes three-surface average except bottom. For the gap size of 0 and 2mm, overall average Nusselt number is highest in the first row and decreases to the fully developed value. But the second row has the highest value in the case of G=5mm. It is interesting to note that chips with only small gap have much higher heat trnasfer values than chips without gap. Furthermore, the present results reveal that front and bottom surfaces can play important roles on the convective heat transfer from electronic chips.

Hexahedral element, which is 30mm wide, 60mm long and 10mm high, is used for the experiments of three-dimensional chip array. Recess of 1.5mm is provided on three surfaces (front, top and rear) of the element to hold the naphthalene except near the edge of 5mm (Fig. 9). Fifteen elements, five rows and three columns, are

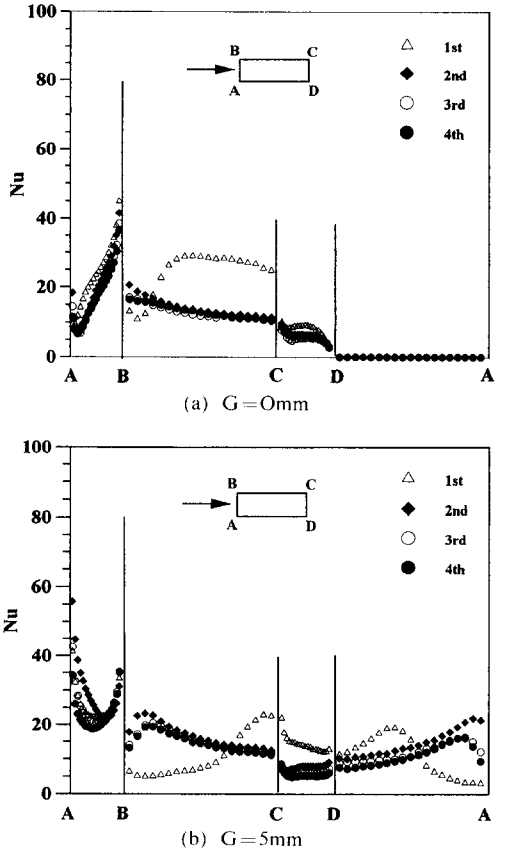

Fig. 7 Effect of chip position on heat transfer for 2D chip array (u=5m/s)

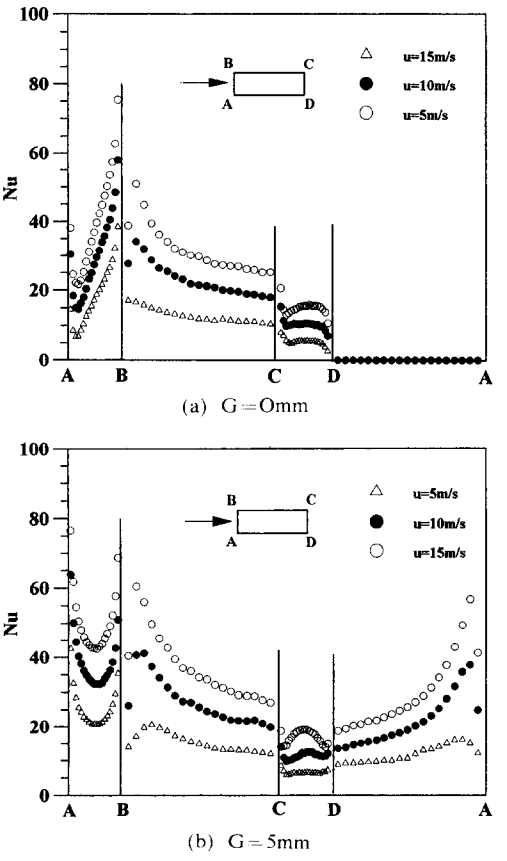

Fig. 8 Effect of inlet velocity on heat transfer for 2D chip array (3rd chip)

Table 1 Effect of gap size on average Nusselt number for 2D array (u=5m/s)

G(mm)	Row	Front	Bottom	Rear	Top	Overall
0	1	33	—	11	34	18(29)
	2	29	—	8	20	12(19)
	3	26	—	7	18	11(18)
	4	25	—	8	18	11(17)
2	1	39	12	17	17	18
	2	31	11	6	20	16
	3	32	10	6	19	16
	4	30	10	6	18	15
5	1	37	20	20	15	18
	2	43	11	11	23	23
	3	37	9	9	21	20
	4	33	8	8	20	18

mounted on the same flow channel and the wind tunnel that is used in the measurement of 2D chip array, as shown in Fig. 10. Only one element is naththalene active and the others are dummy elements made of arcryl. Geometric variable is streamwise spacing (S) between adjacent chips and other dimensions are held fixed during the experiments.

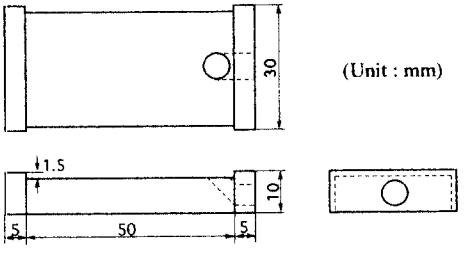

Fig. 9 Schematic of testpiece - 3D simulated chip

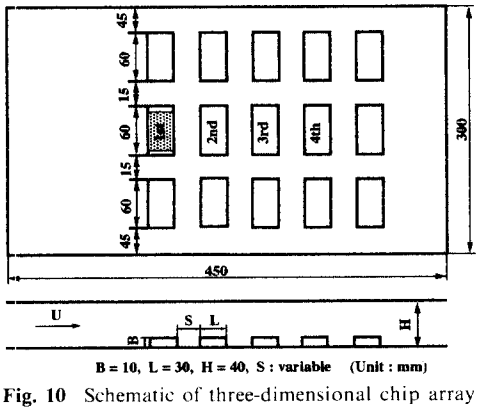

Fig. 10 Schematic of three-dimensional chip array

Figure 11 shows 3D view of the local Nusselt number distribution. Three dimensionality is seen on the bottom edge of the front surface. Bypass flow through spanwise chips penetrate into a wake region between streamwise chips and interact with the cavity flow. This penetration is deeper as the streamwise chip spacing increases. More distinct penetration effect is seen on the rear surface (Fig. 12), but little influence is found on the top surface. Distributions of spanwise-average of the local heat transfer coefficients in the three-dimensional chip array are presented in Fig. 13, and they are compared with those measured in the two-dimensional array. Variation trends are much similar regardless of chip spacing and dimensionality. But, in the case of three-dimensional array, higher values are observed on all surfaces of S/L = 1 and on the front and rear surfaces of S/L = 0.5 than two-dimensional array. Little difference is seen on the chip of S/L = 0.25. The source of discrepancy between 2D and 3D is considered as the interaction of the cavity flow with the bypass flow, as mentioned in the discussion of local heat transfer distribution. The oeverall average Nuselt numbers are compared in Table 2 for various chip spacings and air velocities. Overall average values are measured using four different methods. Weighing denotes overall average measured by the weighing method, and local denotes overall average obtained by integrating local

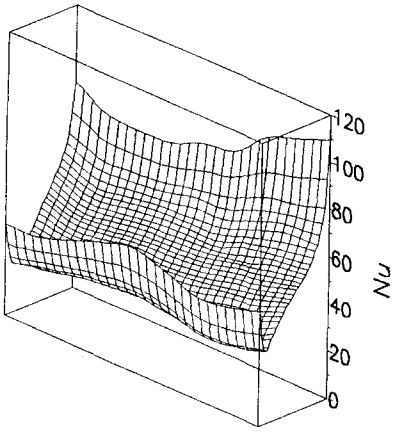

(a) S/L=1

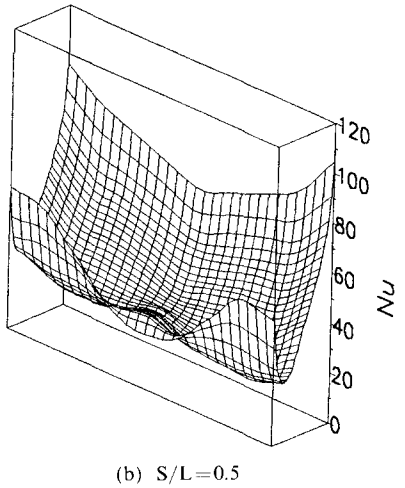

(b) S/L=0.5

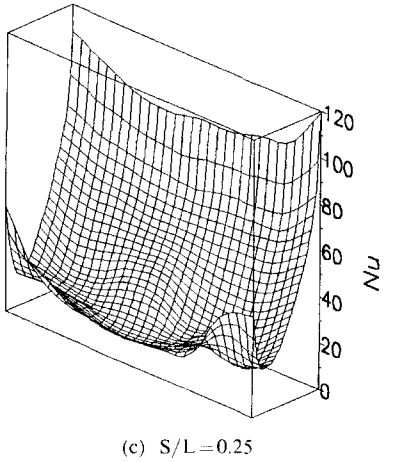

(c) S/L=0.25

Fig. 11 Effect of streamwise chip spacing on heat transfer for 3D chip array (front surface, u=5m/s)

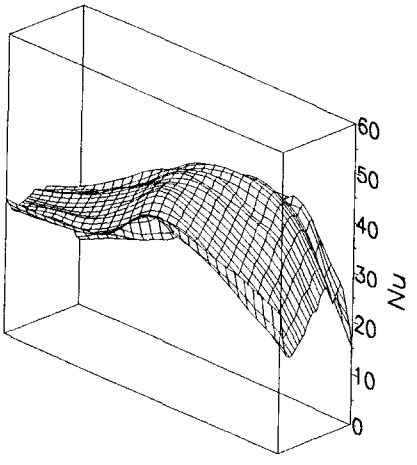

(a) S/L=1

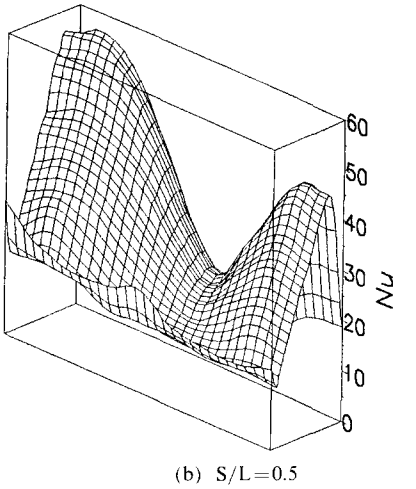

(b) S/L=0.5

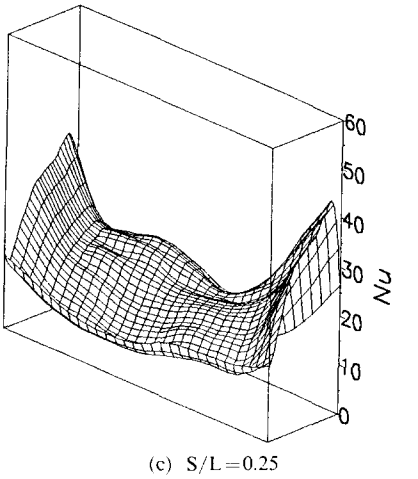

(c) S/L=0.25

Fig. 12 Effect of streamwise chip spacing on heat transfer for 3D chip array (rear surface, u=5m/s)

values. 2D represents two-dimensional array, while 3D represents three-dimensional array and all six surfaces of hexahedral chip are casted with naphthalene in the case of cake. There are only minor deviations among the values of 3D-weighing, cake and 3D-local, while overall aver-

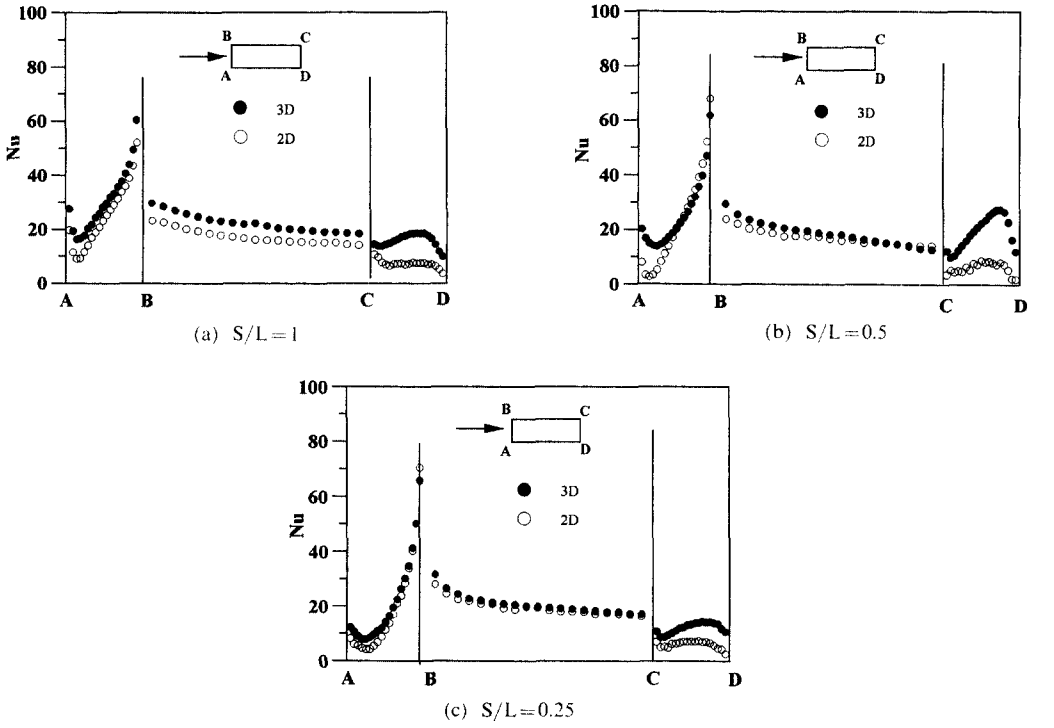

(a) S/L=1 (b) S/L=0.5

(c) S/L=0.25

Fig. 13 Comparison of local Nusselt number for 2D and 3D chip arrays (u=5m/s)

Table 2 Comparison of average Nusselt numbers for 2D and 3D chip arrays

S/L	Velocity (m/s)	Row	Weighing		Local	
			3D	Cake	3D	2D
1	5	1st	30	30	31	29
		2nd	23	24	25	20
		3rd	22	23	23	18
	10	1st	46	49	47	46
		2nd	39	40	43	40
		3rd	38	40	39	31
	15	1st	55	58	61	58
		2nd	49	52	54	49
		3rd	49	50	54	42
0.5	5	1st	31	34	31	32
		2nd	26	25	28	24
		3rd	24	24	23	22
0.25	5	1st	28	34	28	30
		2nd	22	22	20	20
		3rd	21	21	19	17

age heat transfer coefficients on the two-dimensional chip array (2D-local) are lower than those of three-dimensional chip array (3D-local). Differences in the magnitude decrease as the longitudinal chip spacing decrease.

5. Conclusions

Detailed measurements of the local and average mass transfer for single chip, two-dimensional chip array and three-dimensional chip array are performed using a naphthalene sublimation technique. Mass transfer data are converted to their counterpart of heat transfer using the heat/mass transfer analogy. Summary of major results are as follows.

① Dramatic change of the local heat transfer distribution is seen on each surface of the chip, and gap size between chip and base plate is found to affect the local heat transfer characteristics significantly.

② Chips with small gap have much higher heat transfer values than chips without gap. This reveals that front and bottom surfaces of electronic chips can play an important role on the convective heat transfer.

③ In the case of three dimensional modules, interaction of the cavity flow with the bypass flow influneces the heat transfer. As the result of this interaction, three dimensionalities is seen on the front of rear surface.

④ Local and average heat transfer coefficients of three-dimensional modules are a little bit higher than those of two-dimensional modules. Differences in magnitude decrease as the streamwise chip spacing decreases.

Acknowledgment

This study was financially supported by Korea Science and Engineering Foundation (KOSEF) under Grant number of 921-0900-017-2. Authors gratefully appreciate the support.

References

Ambrose, D., Lawrenson, I.J. and Sparke, C.H. S., 1975, "The Vapor Pressure of Naphthalene," *Journal of Chemical Thermodynamics,* Vol. 7, pp. 1173~1176.

Cho, K., 1989, "Measurement of Diffusion Coefficient of Naphthalene into Air," Ph. D Thesis, State University of New York.

Chyu, M.K. and Natarajan, V., 1991, "Local Heat/Mass Transfer Distributions on the Surface of a Wall-Mounted Cube," ASME *Journal of Heat Transfer,* Vol. 113, pp. 851~857.

Goldstein, R.J., Yoo, S.Y. and Chung, M.K., 1990, "Convective Mass Transfer from a Square Cylinder and Its Base Plate," *International Journal of Heat and Mass Transfer,* Vol. 33, pp. 9~18.

Perterson, G.P. and Ortega, A., 1990, "Thermal Control of Electronic Equipment and Devices," *Advances in Heat Transfer,* Vol. 20, pp. 181~314.

Sparrow, E. M., Vemuri, S. B. and Kadle, D. S., 1983, "Enhanced and Local Heat Transfer, Pressure Drop and Flow Visualization for Arrays of Block-Like Electronic Components", *Int. J. of Heat and Mass Transfer,* Vol. 26, pp. 689~699.

Yoo, S. Y., No, J. K., Chung, C. H. and Chung, M. K., 1993, "A Study on the Analogy between Heat Transfer and Mass Transfer," *Transaction of KSME,* Vol. 17, pp. 2624~2633.